Laser Light Scattering Study of a Very Dilute Water/Sodium Bis(2-ethylhexyl)sulfosuccinate/*n*-Hexane Microemulsion Stabilized by Poly(*N*-isopropylacrylamide)

Shuiqin Zhou and Chi Wu*

Department of Chemistry, The Chinese University of Hong Kong, Shatin, N.T., Hong Kong

Received November 17, 1994; Revised Manuscript Received May 5, 1995[⊗]

ABSTRACT: The "water-in-oil" microemulsion polymerization of (*N*-isopropylacrylamide) (NIPAM) enabled us to prepare a series of dilute "water/sodium bis(2-ethylhexyl)sulfosuccinate (AOT)/*n*-hexane" microemulsions with PNIPAM as a stabilizer. A combination of static and dynamic laser light scattering (LLS) was used to study the temperature (T) and dispersed-phase concentration (C) dependence of this series of dilute microemulsions. For a given water/AOT molar ratio of $\omega = 23$, the average hydrodynamic radius ($\langle R_h \rangle$) of the microemulsion increases with T when C is higher than 0.150 g/mL but decreases when C is ~100-fold dilute. In comparison with the H_2O/AOT/*n*-hexane microemulsion wherein no PNIPAM is introduced as a stabilizer, the H_2O(PNIPAM)/AOT/*n*-hexane microemulsion is much more stable in the range of $1.50 \times 10^{-3} \leq C \leq 7.50 \times 10^{-3}$ g/mL. On the basis of a spherical core–shell model, i.e., a water core coated with a layer of AOT, we determined the AOT layer thickness (b) from the difference between the hydrodynamic radius (R_h) measured in dynamic LLS and the radius of the water core (R_c) calculated from the mass (M_w) of the water core obtained in static LLS, i.e., $b = R_h - R_c$. The estimate of $b \sim 1.1$ nm indicates that the water core is covered with only one monolayer of AOT molecules and the AOT molecules stand right on the surface of the water core, which is quite different from our previously reported model for the "oil-in-water" microemulsion, wherein half of the surfactant hydrophobic tail penetrates into the core.

Introduction

Microemulsions consist of a thermodynamically stable, transparent, and homogeneous single-phase solution of oil, water, and surfactants. For water-in-oil, it is widely accepted that the microemulsion is a fine dispersion of surfactant-coated water droplets (with a diameter of ~10 nm) in a continuous oil phase.[1–4] The formation and property of a given microemulsion depend on many factors, such as temperature, concentration, and the nature of each existing component.[5] Oakenfull[6] showed that when the ratio of V/L is larger than 0.7, the water/oil interface will have a tendency to bend to form a water-in-oil microemulsion with the hydrophilic head of the surfactant facing toward the center of the water droplet, where V and L are the volume of the head and the length of the surfactant hydrophobic tail, respectively. Sodium bis(2-ethylhexyl)sulfosuccinate (AOT) with $V/L > 0.7$ can spontaneously bend to form a water-in-oil microemulsion without any additional cosurfactants.[7] Using AOT as a surfactant can minimize the number of chemical components in the preparation of a microemulsion. This is why AOT has been widely used as a surfactant in the "water-in-oil" microemulsion.

The H_2O/AOT/oil microemulsion has been extensively studied.[8–12] Most studies involved relatively concentrated microemulsions because the dilute H_2O/AOT/oil microemulsion is thermodynamically instable. However, a better understanding of the stability and structure of each individual microemulsion droplet requires the study of a very dilute microemulsion wherein the interaction among different droplets can be greatly reduced. Recently, a few experiments were designed to study the H_2O/AOT/oil microemulsions at relatively lower concentrations.[11–13] In this moderate concentration range the size of the droplets is rather uniform and only dependent on the H_2O/AOT molar ratio. Small-angle neutron scattering study[14] showed that, for a given H_2O/AOT molar ratio $\omega = 30$, the size of the droplets decreases dramatically as C decreases in the range of $0.1\% \leq \phi \leq 1\%$, which indicates the emulsification failure. When $\phi < 0.1\%$, no microemulsion droplets can be found in the mixture. Therefore, the study of individual microemulsion droplets in a very dilute concentration is impossible.

On the other hand, the interaction between polymers and the microemulsions has attracted much attention in both basic research and industrial applications. Candau et al.[15] polymerized acrylamide in the H_2O/AOT/toluene microemulsion. Laser light scattering (LLS) and viscosity data showed that polyacrylamide acted as a cosurfactant and partially located at the H_2O/toluene interface between the hydrophobic tails of AOT.[16] Further, the interaction between poly(*N*-isopropylacrylamide) (PNIPAM) and surfactant was studied. It was found that the presence of PNIPAM has a promotive effect on the micellization of sodium *n*-alkylsulfate ($n \geq 5$).[17–20] Later, Pelton[21] found that the polystyrene latex prepared with only SDS was unstable in dialysis, while a small amount of added PNIPAM would lead ot a much more stable colloid.

This study has two objectives. The first is to prepare a stable and dilute water-in-oil microemulsion by polymerizing NIPAM inside the water core, so that we can study individual microemulsion droplets with minimum interdroplet interactions. The second is to develop an LLS method to study the structure of spherical water-in-oil microemulsion droplets since LLS is more available than small-angle neutron scattering. In previous studies, we have used a combination of static and dynamic LLS to get some important structure parameters of the "oil-in-water" microemulsions.[22,23]

Basic Theories

Static Laser Light Scattering (LLS). The angular dependence of the excess absolute time-averaged scat-

[⊗] Abstract published in *Advance ACS Abstracts,* June 15, 1995.

0024-9297/95/2228-5225$09.00/0

tered intensity, known as Rayleigh ratio $R_{vv}(q)$, is measured. For a dilute solution, $R_{vv}(q)$ can be expressed as[24]

$$\frac{KC}{R_{vv}(q)} \approx \frac{1}{M_w}\left(1 + \frac{1}{3}\langle R_g^2\rangle q^2\right) + 2A_2C \quad (1)$$

where $K = 4\pi n^2(dn/dC)^2/(N_A\lambda^4)$ and $q = (4\pi n/\lambda)\sin(\theta/2)$ with n, dn/dC, N_A, λ, and θ being the solvent refractive index, the differential refractive index increment, Avogadro's number, the wavelength of the incident light in vacuo, and the scattering angle, respectively. By measuring $R_{vv}(q)$ at a set of C and θ, we can determine M_w, R_g, and A_2 from a Zimm plot which incorporates the C and q dependence of $KC/R_{vv}(q)$ in a single grid.[24]

Dynamic LLS. The intensity–intensity time correlation function $G^{(2)}(t,q)$ in the self-beating mode is measured. $G^{(2)}(t,q)$ can be related to the electric field time correlation function $g^{(1)}(t,q)$ as[25,26]

$$G^{(2)}(t,q) = \langle I(t,q)\, I(0,q)\rangle = A[1 + \beta|g^{(1)}(t,q)|^2] \quad (2)$$

where A is the baseline; β, a parameter depending on the coherence of the detection; and t, the delay time. $g^{(1)}(t,\theta)$ is further related to the characteristic line-width (Γ) distribution $G(\Gamma)$ by

$$g^{(1)}(t,q) = \langle E(t,q)\, E^*(0,q)\rangle = \int_0^\infty G(\Gamma)\, e^{-\Gamma t}\, d\Gamma \quad (3)$$

$G(\Gamma)$ can be calculated from a Laplace inversion of $G^{(2)}(t,q)$ on the basis of eqs 2 and 3. If the relaxation is diffusive, Γ can be related to the translational diffusion coefficient D as[27]

$$\Gamma/q^2 = D(1 + k_dC)(1 + f\langle R_g^2\rangle q^2) \quad (4)$$

where k_d is the diffusion second virial coefficient, and f, a dimensionless number related to the hydrodynamic draining, the internal motion, and the solvent quality. Both of the thermodynamic and hydrodynamic interactions contribute to k_d as[28]

$$k_d = 2A_2M_w - \frac{C_DN_AR_h^3}{M_w} \quad (5)$$

where C_D is an empirical positive constant, and R_h, the hydrodynamic radius related to D by the Stokes–Einstein equation, $R_h = k_BT/6\pi\eta D$, with T, k_B, and η being the absolute temperature, the Boltzmann constant, and the solvent viscosity, respectively. Therefore, $G(\Gamma)$ can be converted into either the translational diffusion coefficient distribution $G(D)$ or the hydrodynamic radius distribution $f(R_h)$.

Experimental Section

Materials. *N*-Isopropylacrylamide (NIPAM) purchased from Kodak was purified by a three-time recrystallization in a benzene/hexane mixture. Sodium bis(2-ethylhexyl)sulfosuccinate (AOT; from Sigma, 99%) as a surfactant, potassium persulfate ($K_2S_2O_8$; from Aldrich, analytical grade) as an initiator, and *N,N,N′,N′*-tetramethylenediamine (TEMED; from Fluka) as an accelerator were used without further purification. Freshly distilled and deionized water was used for all sample preparation. *n*-Hexane (from Aldrich, analytical grade) as a dispersion medium was distilled just before use. It should be noted that *n*-hexane instead of decane was used here because it is known that short-chain oil molecules can pack favorably with the surfactant's hydrophobic tail.[2]

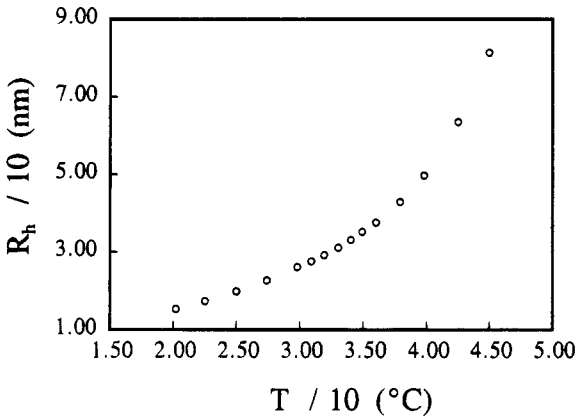

Figure 1. Temperature dependence of the average hydrodynamic radius $\langle R_h\rangle$ for a concentrated H_2O(PNIPAM)/AOT/*n*-hexane microemulsion, where $C = 0.150$ g/mL and $\omega = 23$.

Table 1. Summary of Dynamic LLS Results of the H_2O (PNIPAM)/AOT/*n*-Hexane at Different Concentrations (C), Temperatures (T), and Scattering Angles (θ)

		T = 25.02 °C		T = 34.64 °C	
C/(g/mL)	θ	$\langle R_h\rangle$/nm	$\mu_2/\langle\Gamma\rangle^2$	$\langle R_h\rangle$/nm	$\mu_2/\langle\Gamma\rangle^2$
0.150	30°	21.0	0.04	36.7	0.05
	90°	23.5	0.04	37.2	0.04
0.00150	15°	4.50	0.05	2.35	0.07
	30°	4.40	0.04		

Sample Preparation. A total of 3.22 g of AOT was dissolved in 40.0 mL of *n*-hexane. Separatively, 0.240 g of NIPAM and 2.5 mg of $K_2S_2O_8$ were dissolved in 3.00 mL of deionized water. Two solutions were mixed, and then the mixture was bubbled with N_2 for 20 min. Finally, 50 μL of TEMED was added to accelerate the polymerization of NIPAM in the water phase. The solution was stirred for 10 h until the polymerization was complete. The dispersed-phase concentration of the final microemulsion was 0.150 g/mL. A successive dilution of this stock microemulsion with *n*-hexane led to five dilute H_2O(PNIPAM)/AOT/*n*-hexane microemulsions, with the dispersed-phase concentration (C) being 1.5, 3.0, 4.5, 6.0, and 7.5 mg/mL, where the water/AOT molar ratio was fixed on $\omega = 23$.

LLS Measurements. A commercial LLS spectrometer (ALV/sp-125, Langan in Hessen, Germany) equipped with an ALV-5000 multi-τ digital time correlator was used. The light source was a vertically polarized Nd:YAG laser operated at 532 nm and 400 mW (Adlas GmbH & Co. KG, Germany). Time correlation functions were analyzed by the Laplace inversion program (CONTIN) equipped with the correlator. The detail of the LLS instrumentation can be found elsewhere.[25,26] In static LLS, a precise value of the differential refractive index increment (dn/dC) is vital for the absolute scattering intensity measurement. Therefore, we used a novel differential refractometer to determine the dn/dC of the H_2O-(PNIPAM)/AOT/*n*-hexane microemulsion.[29] It should be noted that in both the static LLS and dn/dC measurements *n-hexane with the same amount of added AOT as in the microemulsion was used as the reference solvent so that the light scattered and refracted from AOT was experimentally compensated.* Such determined dn/dC was 0.0546 cm³/g at T = 25 °C and λ = 532 nm.

Results and Discussion

Figure 1 shows the temperature dependence of the average hydrodynamic radius $\langle R_h\rangle$ of the stock H_2O-(PNIPAM)/AOT/*n*-hexane microemulsion, where $\langle R_h\rangle = \int_0^\infty R_h f(R_h)\, dR_h$, $\theta = 30°$, $C = 0.150$ g/mL, and $\omega = 23$. Dynamic LLS results at different T and θ are summarized in Table 1. The microemulsion has a very narrow size distribution. In the range of 20–45 °C, $\langle R_h\rangle$ increases dramatically with temperature. Our results

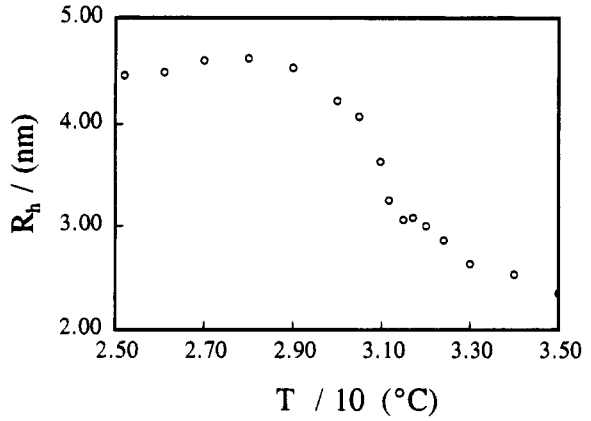

Figure 2. Temperature dependence of the average hydrodynamic radius $\langle R_h \rangle$ for a dilute H_2O(PNIPAM)/AOT/*n*-hexane microemulsion, where $C = 1.50 \times 10^{-3}$ g/mL and $\omega = 23$.

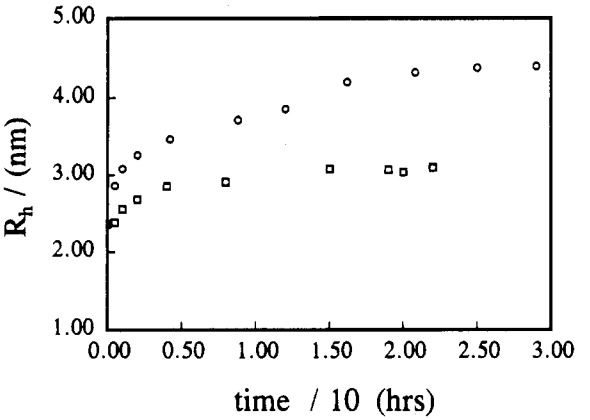

Figure 3. Swelling kinetics of the AOT micelle after T abruptly changed from 35 to 25 °C, where $C = 1.50 \times 10^{-3}$ g/mL and $\omega = 23$: (○) the H_2O(PNIPAM)/AOT/*n*-hexane microemulsion; (□) the H_2O/AOT/*n*-hexane microemulsion.

showed that at all temperatures the relaxation measured in dynamic LLS was diffusive and $\langle\Gamma\rangle/q^2$ (and $\langle R_h \rangle$) is a linear function of q^2 as predicted in eq 4. However, the q dependence of $\langle R_h \rangle$ is not very strong even when $\langle R_h \rangle \sim 80$ nm at $T = 45$ °C because there should be no hydrodynamic draining and internal motions associated with the hard-sphere-like droplets in the microemulsion; i.e., f in eq 4 is very small. The change of $\langle R_h \rangle$ as temperature was completely reversible. We also observed that, for a given temperature, *$\langle R_h \rangle$ did not change with time even at or near the low critical solution temperature (LCST ~ 31 °C) of PNIPAM in water*. This strongly indicates that the microemulsion is thermodynamically stable. The results in Figure 1 agree with those from the H_2O/AOT/isooctane system.[30] The fluorescence study[31] also showed that the mean aggregation number N of the micelle increases with temperature. This T dependence of $\langle R_h \rangle$ was first explained by the assumption that the surfactant shell will lose some surfactant molecules to the inner water core as temperature increases.[30] To restore the same degree of the surfactant coverage on the water core as in a lower T, the droplets have to aggregate with each other to reduce the total surface area. The second explanation of this T dependence of $\langle R_h \rangle$ was in terms of the intermicellar attractive interaction.[9,29] At a high dispersed-phase concentration, the hydrophobic tail of AOT from one droplet will have a chance to interact with the tails of AOT on other droplets. For a thermodynamically stable microemulsion, the surfactant/oil interaction is stronger than the tail/tail interaction. As temperature increases, oil molecules will become less optimally oriented to interact with the tails of AOT, while the tail/tail interaction is less temperature dependent because the tails from two overlap droplets are always more or less parallel to each other. Therefore, the attractive force between two droplets increases with temperature, so that the droplets aggregate and $\langle R_h \rangle$ increases. The above two aggregation mechanisms can be differentiated from the T dependence of $\langle R_h \rangle$ in a very dilute microemulsion, wherein the tail/tail interaction suggested by the second explanation should be greatly suppressed.

Figure 2 shows a plot of $\langle R_h \rangle$ vs T after a 100-fold dilution of the H_2O(PNIPAM)/AOT/*n*-hexane microemulsion used in Figure 1, where $C = 1.50 \times 10^{-3}$ g/mL and $\theta = 15°$. The distribution width $(\mu_2/\langle\Gamma\rangle^2)$ and θ dependence of $\langle R_h \rangle$ are also listed in Table 1. After dilution, the microemulsion is still narrowly distributed and there is no angular dependence of $\langle R_h \rangle$ since the droplet is very small. A comparison of Figures 1 and 2 shows that $\langle R_h \rangle$ decreases dramatically when C changes from 0.150 g/mL to 1.50×10^{-3} g/mL. Therefore, $\langle R_h \rangle$ shown in Figure 1 is apparent. This is exactly why we have to study a very dilute microemulsion. Figure 2 shows that in the range of 25 °C ≤ T ≤ 28 °C $\langle R_h \rangle$ is nearly independent of T, which fits the second explanation because in a very dilute microemulsion the tail/tail interaction between two droplets is so rare that the temperature increase cannot induce aggregation. When $T > 28$ °C, $\langle R_h \rangle$ decreases as temperature increases and finally approaches to a constant value of 2.35 nm which is close to the radius of the AOT micelle in pure *n*-hexane. The sharp decrease in $\langle R_h \rangle$ in the range of 30 °C < T < 31.5 °C might be attributed to the following two reasons. On the one hand, as temperature increases, hexane molecules near the hydrophobic tail of AOT would be less oriented because of the higher thermal energy. In order to stabilize the microemulsion droplets, some water molecules have to be released into the bulk oil phase so that the total surface area of the droplets will reduce and the AOT concentration on the surface of the water core can be maintained. On the other hand, when T approaches the LCST (~31 °C) of PNIPAM in water, the PNIPAM chain will collapse into a globule.[32] As a stabilizer, the PNIPAM globule will lose its cosurfactant role. This is why R_h decreases much fast in the range of 30–31.5 °C.

To verify this stabilizing or cosurfactant effect of PNIPAM, we prepared a H_2O/AOT/*n*-hexane microemulsion with an identical water/AOT molar ratio of $\omega = 23$ and dispersed-phase concentration of $C = 1.50 \times 10^{-3}$ g/mL, but without PNIPAM. In fact, such a H_2O/AOT/*n*-hexane microemulsion was thermodynamically unstable. $\langle R_h \rangle$ of the freshly prepared H_2O/AOT/*n*-hexane microemulsion is 3.61 nm at $T = 25$ °C. At $T = 35$ °C, $\langle R_h \rangle$ decreased to 2.36 nm close to the radius of the AOT micelle in pure *n*-hexane. In Figure 2, the H_2O(PNIPAM)/AOT/*n*-hexane microemulsion has a similar $\langle R_h \rangle$ at $T = 35$ °C. However, the stability of the microemulsion with or without PNIPAM is much different. To demonstrate this difference, we first heated both of the microemulsions to 35 °C and then quenched them from 35 to 25 °C. $\langle R_h \rangle$ was measured as a function of time (t).

Figure 3 shows a plot of $\langle R_h \rangle$ vs t for the H_2O(PNIPAM)/AOT/*n*-hexane (○) and H_2O/AOT/*n*-hexane (□) microemulsions at $C = 1.50 \times 10^{-3}$ g/mL and $T = 25$ °C. For both of the microemulsions $\langle R_h \rangle$ increases with time after T drops from 35 to 25 °C. This clearly

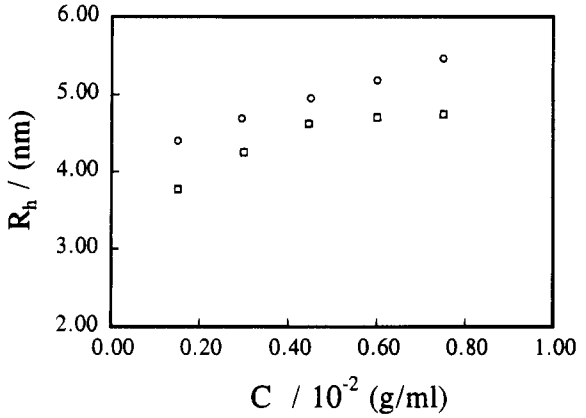

Figure 4. C dependence of the average hydrodynamic radius $\langle R_h \rangle$, where $\omega = 23$ and $T = 25$ °C: (○) the H_2O(PNIPAM)/AOT/*n*-hexane microemulsion; and (□) the H_2O/AOT/*n*-hexane microemulsion.

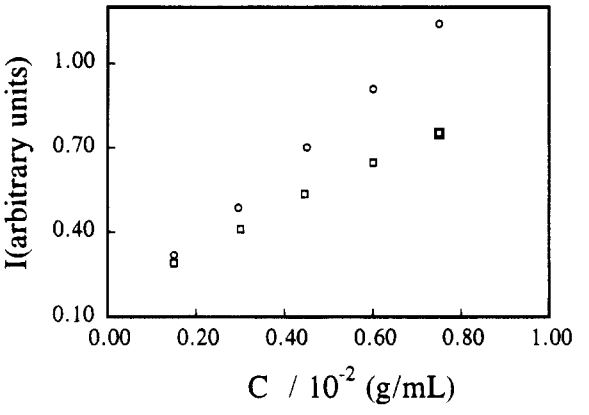

Figure 5. C dependence of scattering intensity (I), where $\omega = 23$, and $T = 25$ °C: (○) the H_2O(PNIPAM)/AOT/*n*-hexane microemulsion; (□) the H_2O/AOT/*n*-hexane microemulsion.

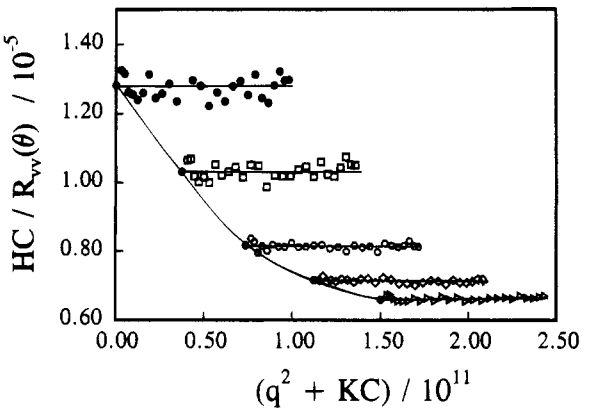

Figure 6. Typical Zimm plot of the H_2O(PNIPAM)/AOT/*n*-hexane microemulsion, where $T = 25$ °C and 1.50×10^{-3} g/mL $\leq C \leq 6.00 \times 10^{-3}$ g/mL.

indicates that the AOT micelle was gradually swollen again by water at 25 °C. In first 2 h, the swelling was fast and then the swelling slowed down at a longer t. After 25 h, the H_2O(PNIPAM)/AOT/*n*-hexane microemulsion reached its stable state and $\langle R_h \rangle$ is the same as before the heating. In contrast, $\langle R_h \rangle$ of the H_2O/AOT/*n*-hexane microemulsion only approaches 3.10 nm, other than its original 3.61 nm. This indicates that the heating and cooling process has brought the H_2O/AOT/*n*-hexane microemulsion an irreversible change. In other words, this path dependence of $\langle R_h \rangle$ shows that the dilute H_2O/AOT/*n*-hexane microemulsion without PNIPAM is thermodynamically unstable at $C = 1.50 \times 10^{-3}$ g/mL.

Figure 4 shows the C dependence of $\langle R_h \rangle$ for the H_2O-(PNIPAM)/AOT/*n*-hexane (○) and H_2O/AOT/*n*-hexane (□) microemulsions, where $T = 25$ ° C and $\theta = 15°$. Without PNIPAM, $\langle R_h \rangle$ is independent of C as long as $C \geq 4.5 \times 10^{-3}$ g/mL, but $\langle R_h \rangle$ drops with dilution when $C < 4.5 \times 10^{-3}$ g/mL. This C dependence of $\langle R_h \rangle$ is similar to those in the H_2O/AOT/decane[14] and H_2O/AOT/isooctane[30] microemulsions. The decrease of $\langle R_h \rangle$ with dilution in a ternary system has been attributed to the phase separation.[14] In contrast, with PNIPAM $\langle R_h \rangle$ is larger than that without PNIPAM at the same concentration, and the decrease of $\langle R_h \rangle$ with dilution is linear. The introduction of PNIPAM in the water core stabilizes the water-in-oil microemulsion in the very dilute region. The slow and linear decrease of $\langle R_h \rangle$ with dilution can be explained in terms of the attractive interaction between the droplets. At a finite concentration, the attractive interaction will slow down the droplet's diffusivity, which leads to a larger apparent $\langle R_h \rangle$. On the basis of eq 4, the extrapolation of $\langle \Gamma/q^2 \rangle$ vs C to infinite dilution leads to a value of $\langle D \rangle_{C \to O} = 1.75 \times 10^{-6}$ cm^2/s and $k_d = -33$ mL/g. From $\langle D \rangle_{C \to O}$, we were able to calculate the true hydrodynamic radius of $\langle R_h \rangle = 4.17$ nm.

Figure 5 shows the scattering intensity (I) as a function of concentration (C) for the H_2O(PNIPAM)/AOT/*n*-hexane (○) and H_2O/AOT/n-hexane (□) microemulsions, where $\theta = 15°$ and $T = 25$ °C. In this dilute region of $1.50 \times 10^{-3} \leq C \leq 7.50 \times 10^{-3}$ (g/mL), the scattering intensity increases linearly with concentration, which is consistent with the results in ref 9. The scattering intensity of the microemulsion with PNIPAM is higher than that of the microemulsion without PNIPAM under the same conditions. This intensity difference (ΔI) can be attributed to the light scattered by PNIPAM molecules ($M_w \approx 6000$) inside the water core. The increase of ΔI with C is due to the fact that the amount of PNIPAM in the H_2O(PNIPAM)/AOT/*n*-hexane microemulsion increases with C. The formation of a series of stable dilute H_2O(PNIPAM)/AOT/*n*-hexane microemulsions enabled us to study it by static LLS.

Figure 6 shows a typical Zimm plot of the H_2O-(PNIPAM)/AOT/*n*-hexane microemulsion, where $\omega = 23$, $T = 25$ °C, and C ranges from 1.50×10^{-3} to 6.00×10^{-3} g/mL. On the basis of eq 1, we were able to calculate $M_w = 7.80 \times 10^4$ from the extrapolation of $[HC/R_{vv}(\theta)]_{\theta \to O, C \to O}$ and $A_2 = -7.95 \times 10^{-4}$ mol·mL/g^2 from $[HC/R_{vv}(\theta)]_{\theta \to O}$ vs C. The size of the droplet is so small that an accurate $\langle R_g \rangle$ cannot be measured. *It should be noted that, in static LLS, $\Delta R(\theta) \propto$ [I(solution) − I(solvent)]. In a water-in-oil microemulsion, I(solution) includes the contributions from the water core, oil, and surfactant. Since we have used a mixture of oil and AOT as the reference solvent, $\Delta R(\theta)$ in Figure 6 represents the net light intensity scattered only from the water core; namely, the influence of AOT in the microemulsion has been experimentally compensated.* Here, M_w is the weight-average mass of the water core. The negative A_2 indicates that *n*-hexane is a poor solvent even though the droplets are protected with AOT and stabilized by PNIPAM. The negative A_2 in static LLS agrees well with the negative k_d in dynamic LLS according to eq 5. The change of $[HC/R_{vv}(\theta)]_{\theta \to O}$ vs C agrees well with the static structure factor $S(\phi)$ vs the dispersed-phase volume fraction ϕ obtained by Dozier et al.[12] Their results also showed a negative virial coefficient and a

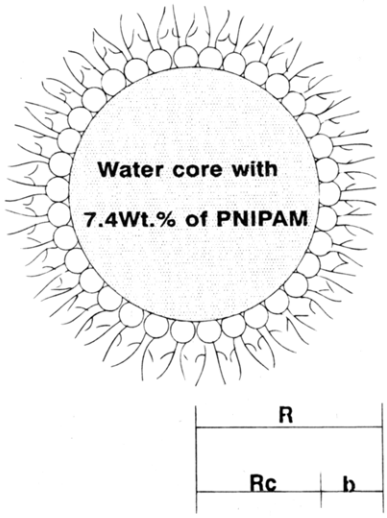

Figure 7. Schematic of a spherical core–shell structural model for the H_2O(PNIPAM)/AOT/n-hexane microemulsion.

linear dependence of $S(\phi)$ on ϕ when the microemulsion is dilute.

Figure 7 shows a spherical core–shell model for the water-in-oil microemulsion. On the one hand, for the narrowly distributed microemulsion droplets, M_w obtained in Figure 6 can lead to an average radius ($\langle R_c \rangle$) of the water core by using $M_w = {}^4/_3\,\pi R_c^3 \varrho N_A$, where ϱ is the water density (~1.0 g/cm^3). On the other hand, we know that $\langle R_h \rangle_{C \to 0} = 4.17$ nm in Figure 4. The difference between $\langle R_h \rangle$ and $\langle R_c \rangle$ is the surfactant shell thickness (b), i.e., $b = \langle R_h \rangle - \langle R_c \rangle = 4.17 - 3.07 = 1.10$ nm which is very close to the length of an AOT molecule (~1.2 nm) calculated from its known chemical structure.[33]

Conclusions

Poly(*N*-isopropylacrylamide) (PNIPAM) can be polymerized inside the small water droplets in a water-in-oil microemulsion. The introduction of PNIPAM can stabilize the microemulsion. Therefore, we were able to prepare a series of dilute H_2O/AOT/n-hexane microemulsions in the range of 1.50×10^{-3} g/mL $\le C \le 7.50 \times 10^{-3}$ g/mL. The laser light scattering (LLS) results showed that the H_2O/AOT/n-hexane microemulsion with PNIPAM is thermodynamically stable even at a very dilute dispersed-phase concentration (~1×10^{-3} g/mL), while the microemulsion without PNIPAM is unstable under the same conditions. When the microemulsion is dilute, such as $C = 1.50 \times 10^{-3}$ g/mL, the average hydrodynamic radius $\langle R_h \rangle$ of the droplets decreases as temperature increases, while at a higher concentration of $C = 0.150$ g/mL, $\langle R_h \rangle$ increases with temperature. This reflects a stronger interaction among the droplets in the microemulsion if the concentration is high. Therefore, all parameters obtained from a concentrated microemulsion should be apparent. The conclusions based on these apparent parameters in the past should be reexamined. A combination of $\langle R_h \rangle$ from dynamic LLS and M_w from statis LLS enabled us to determine the thickness (b) of the surfactant shell to be ~1.1 nm which is very close to the length of a AOT molecule. This suggests that the structure of the H_2O(PNIPAM)/AOT/n-hexane microemulsion can be modeled as a spherical core–shell model, wherein the water core is coated with only one monolayer of AOT molecules standing on the surface of the water core.

Acknowledgment. We gratefully acknowledge the financial support of this work by the Earmarked Research Grant (221600260), the Research Grants Council of the Hong Kong Government.

References and Notes

(1) Napper, D. H. *Polymeric Stabilizers of Colloidal Dispersants*; Academic Press: London, 1983.
(2) Kotlarchyk, M.; Chen, S. H.; Huang, J. S.; Kim, M. W. *Phys. Rev. A* **1984**, *29*, 2054.
(3) Kaler, E. W.; Bennett, K. E.; Davis, H. T.; Scriven, L. E. *J. Chem. Phys.* **1983**, *79*, 5673.
(4) Kotlarchyk, M.; Stephens, R. B.; Huang, J. S. *J. Phys. Chem.* **1988**, *92*, 1533.
(5) John, A. C.; Rakshit, A. K. *J. Colloid Interface Sci.* **1993**, *156*, 202.
(6) Oakenfull, D. *J. Chem. Soc., Faraday Trans 1* **1980**, *76*, 1875.
(7) Rosen, M. J. *Structure/Performance Relationships in Surfactants*; ACS Symposium Series 253, American Chemical Society: Washington, DC, 1984; p 153.
(8) Kotlarchyk, M.; Chen, S. H.; Huang, J. S.; Kim, M. K. *Phys. Rev. Lett.* **1984**, *53*, 941.
(9) Huang, J. S. *J. Chem. Phys.* **1985**, *82*, 480.
(10) Huang, J. S.; Sung, J.; Wu, X. L. *J. Colloid Interface Sci.* **1989**, *132*, 34.
(11) Kim, M. W.; Dozier, W. D.; Klein, R. *J. Chem. Phys.* **1986**, *84*, 5919.
(12) Dozier, W. D.; Kim, M. W. *J. Chem. Phys.* **1987**, *87*, 1455.
(13) Chen, S. H.; Lin, T. L.; Huang, J. S. In *Physics of Complex and Supermolecular Fluids*; Safran, S. A., Clark, N. A. Eds.; John Wiley & Sons: New York, 1987; p 285.
(14) Wu, X. L.; Tong, P.; Huang, J. S. *J. Colloid Interface Sci.* **1992**, *148*, 104.
(15) Candau, F.; Leong, Y. S. *J. Polym. Sci., Polym. Chem. Ed.* **1985**, *23*, 193.
(16) Leong, Y. S.; Candau, S.; Candau, F. In *Surfactants in Solution*; Mittal, K. L., Lindman, B., Eds.; Plenum: New York, 1984; Vol. 3, p 1897.
(17) Goddard, E. D. *Colloid Surf.* **1986**, *19*, 255.
(18) Sundrama, K. K. *Photochemistry in Microheterogeneous Systems*; Academic Press: New York, 1987.
(19) Schild, H. G.; Tirrell, D. A. *Polym. Prepr. (Am. Chem. Soc., Div. Polym. Chem.)* **1989**, *30* (2), 350.
(20) Schild, H. G.; Tirrell, D. A. *Langmuir* **1991**, *7*, 665.
(21) Pelton, R. H. *J. Polym. Sci., Part A: Polym. Chem. Ed.* **1988**, *26*, 9.
(22) Wu, C. *Macromolecules* **1994**, *27*, 298.
(23) Wu, C. *Macromolecules* **1994**, *27*, 7099.
(24) Zimm, B. H. *J. Chem. Phys.* **1948**, *16*, 1099.
(25) Chu, B. *Laser Light Scattering*; Academic Press: New York, 1974.
(26) Pecora, R. *Dynamic Light Scattering*; Plenum Press: New York, 1976.
(27) Stockmayer, W. H.; Schidt, M. *Pure Appl. Chem.* **1982**, *54*, 407; *Macromolecules* **1984**, *17*, 509.
(28) Yamakawa, H. *Modern Theory of Polymer Solution*; Harper and Row: New York, 1971.
(29) Wu, C.; Xia, K. Q. *Rev. Sci. Instrum.* **1994**, *65*, 587.
(30) Zulauf, M.; Eicke, H. F. *J. Phys. Chem.* **1979**, *83*, 480.
(31) Lang, J.; Jada, A.; Malliaries, A. *J. Phys. Chem.* **1988**, *92*, 1946.
(32) Fujishinge, S.; Kubota, K.; Ando, I. *J. Phys. Chem.* **1989**, *93*, 3311.
(33) Eicke, H. F.; Arnold, V. *J. Colloid Interface Sci.* **1974**, *46*, 101. Eicke, H. F.; Shepherd, J. C. W. *Helv. Chim. Acta* **1974**, *57*, 1951.

MA946305D